

Valence evaluation of LiMnO_2 and related battery materials by x-ray absorption spectroscopy

H. Wadati,^{1,*} D. G. Hawthorn,² T. Z. Regier,³ G. Chen,⁴
T. Hitosugi,⁵ T. Mizokawa,⁶ A. Tanaka,⁷ and G. A. Sawatzky¹

¹*Department of Physics and Astronomy, University of British Columbia, Vancouver, British Columbia V6T 1Z1, Canada*

²*Department of Physics and Astronomy, University of Waterloo, Waterloo, Ontario N2L 3G1, Canada*

³*Canadian Light Source, University of Saskatchewan, Saskatoon, Saskatchewan S7N 0X4, Canada*

⁴*Department of Materials Science, College of Materials Science and Engineering,
Jilin University, Changchun 130012, People's Republic of China*

⁵*WPI Advanced Institute for Materials Research (WPI-AIMR), Tohoku University, Sendai 980-8577, Japan*

⁶*Department of Complexity Science and Engineering,
University of Tokyo, Kashiwa, Chiba 277-8561, Japan*

⁷*Department of Quantum Matters, ADSM, Hiroshima University, Hiroshima 739-8530, Japan*

(Dated: October 22, 2018)

We present an x-ray absorption study of the oxidation states of transition-metal-ions of LiMnO_2 and its related materials, widely used as cathodes in Li-ion batteries. The comparison between the obtained spectrum and the configuration-interaction cluster-model calculations showed that the Mn^{3+} in LiMnO_2 is a mixture of the high-spin and low-spin states. We found that Li deficiencies occur in the case of Cr substitution, whereas there are no Li deficiencies in the case of Ni substitution. We conclude that the substitution of charge-transfer-type Ni or Cu is effective for LiMnO_2 battery materials.

Many current electrodes of rechargeable Li batteries have layered structures. Among them, a layered transition-metal oxide Li_xCoO_2 , in which the concurrent insertion of Li in a crystal structure and the reduction of the Co ions is achieved [1], has become widely used as a cathode electrode in the batteries in most portable electronics. Since then, much effort has been made to enhance charge/discharge rates of the cathode material and/or to replace Li_xCoO_2 by less expensive Li_xMnO_2 or related materials. In addition, in the recent ab-initio computational modeling study, $\text{LiNi}_{0.5}\text{Mn}_{0.5}\text{O}_2$ is proposed as a next generation cathode material with high power and high capacity applications [2]. Although the valence states and local electronic configurations of the transition-metal ions are related to the charge/discharge rates, no systematic spectroscopic study has been performed to identify their local electronic configurations experimentally. Here, we report a systematic x-ray absorption spectroscopy (XAS) study of LiMnO_2 , $\text{LiNi}_{0.5}\text{Mn}_{0.5}\text{O}_2$, and related compounds which are thought as future cathode materials. The present experiment and theoretical analysis reveal that LiMnO_2 has the Mn^{3+} site with the unexpected degeneracy between the low-spin (LS) and high-spin (HS) states and that $\text{LiNi}_{0.5}\text{Mn}_{0.5}\text{O}_2$ consists of HS Ni^{2+} and Mn^{4+} . In the case of LiMnO_2 , small perturbation such as Cr doping may stabilize the LS Mn^{3+} state. These results show the potential of LiMnO_2 and $\text{LiNi}_{0.5}\text{Mn}_{0.5}\text{O}_2$ for use as cathode materials and provide fundamental information that can be used for the development of new Li-ion batteries for high power applications.

LiCoO_2 , LiMnO_2 , and $\text{LiNi}_{0.5}\text{Mn}_{0.5}\text{O}_2$ have the layered structure as schematically shown in Fig. 1 (a). In

this structure, the O^{2-} ions provide a framework with face-centered cubic structure and Li^+ and transition-metal ions occupy all the octahedral interstices, leading to alternate two-dimensional triangular lattice layers. Under the octahedral crystal field, the five-fold transition-metal 3d level is split into two-fold e_g and three-fold t_{2g} levels. In these layered cathode materials, the Li^+ ions diffuse between the octahedral sites through the tetrahedral interstices. In LiCoO_2 , the pathways of Li^+ ions are in contact with the LS Co^{3+} in which the t_{2g} orbitals are fully occupied (t_{2g}^6). After the charging process, the LS Co^{3+} (t_{2g}^6) is partly changed into the LS Co^{4+} (t_{2g}^5), in which the structural change by the oxidation is minimal. The electronic configurations of these two Co ions are shown in Fig. 1 (b). If the Mn^{3+} ion in LiMnO_2 and the Mn^{4+} ion after the charging process take the electronic configurations of LS t_{2g}^4 and t_{2g}^3 , respectively, as recently indicated by ab-initio calculation [3], the structural change by the oxidation is also expected to be minimal. If the Mn^{3+} ion in LiMnO_2 takes the HS configuration with one e_g electron, the Mn octahedral site should be deformed by Jahn-Teller effect to lift the two-fold degeneracy of the e_g levels. In such case, local structural change during the charging process is substantial, leading to poor charge/discharge rate as well as poor charge/discharge cycle lifetime. The electronic configurations of these three Mn ions are shown in Fig. 1 (c). In $\text{LiNi}_{0.5}\text{Mn}_{0.5}\text{O}_2$, half of the Li^+ activated sites are in contact with Ni^{2+} and higher Li diffusivity is expected. If the Ni^{2+} ion in $\text{LiNi}_{0.5}\text{Mn}_{0.5}\text{O}_2$ and the Ni^{4+} ion after the charging process take the HS configuration $t_{2g}^6e_g^2$ and the LS configuration t_{2g}^6 , respectively, both of these ions are Jahn-Teller inactive.

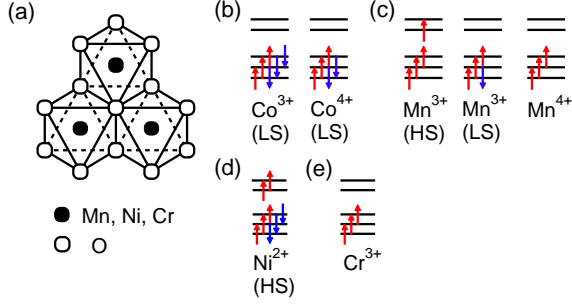


FIG. 1: (Color online) Crystal structure of cathode materials (a) and electronic configurations. (b) Co³⁺ (LS) and Co⁴⁺ (LS). (c) Mn³⁺ (HS), Mn³⁺ (LS) and Mn⁴⁺. (d) Ni²⁺ (HS). (e) Cr³⁺.

As discussed in the previous paragraph, the local electronic configuration of the transition-metal ions is highly important to determine the electrochemical properties of the cathode materials. In this report, we present a systematic XAS study of the cathode materials to extract fundamental information on their electronic configurations. We determined the valence of transition-metal ions by XAS and discussed what type of substitution is most suitable for LiMnO₂ batteries.

The powder samples of LiMnO₂, LiMn_{0.5}Ni_{0.5}O₂, and LiMn_{0.65}Cr_{0.35}O₂ were synthesized by the procedure described in Refs. [3, 4]. The powder of LiMnO₂ and LiMn_{0.5}Ni_{0.5}O₂ have a monoclinic structure, while LiMn_{0.65}Cr_{0.35}O₂ has a rhombohedral (α -NaFeO₂-type) one. XAS experiments were performed at 11ID-1 (SGM) of the Canadian Light Source. The spectra were measured in the total-electron-yield (TEY) mode. The obtained TEY spectra were similar to the partial-fluorescence-yield spectra. The resolution power ($E/\Delta E$) was set to 5000. All the spectra were measured at room temperature.

Figure 2 (a) shows the Mn 2*p* XAS spectra and their comparison with the reference data of Mn²⁺ (MnO), Mn³⁺ (LaMnO₃), and Mn⁴⁺ (EuCo_{0.5}Mn_{0.5}O₃ and SrMnO₃) from Ref. [5]. The spectra of LiMn_{0.5}Ni_{0.5}O₂ and LiMn_{0.65}Cr_{0.35}O₂ are very similar to those of the Mn⁴⁺ references, indicating that the valence of Mn is 4+ in these materials. The spectrum of LiMnO₂ is different from the other three results and also from the Mn²⁺ and Mn⁴⁺ references. It is similar to the Mn³⁺ reference of LaMnO₃, but the lineshapes are slightly different. We considered that this difference may come from the spin states, that is the difference between HS and LS states, and performed configuration-interaction (CI) cluster-model calculations [6]. Figure 2 (b) shows the comparison with the CI theory. The value of the crystal field splitting between *e_g* and *t_{2g}* states, 10*Dq*, was changed from 1.0 eV to 2.0 eV. The positive value of

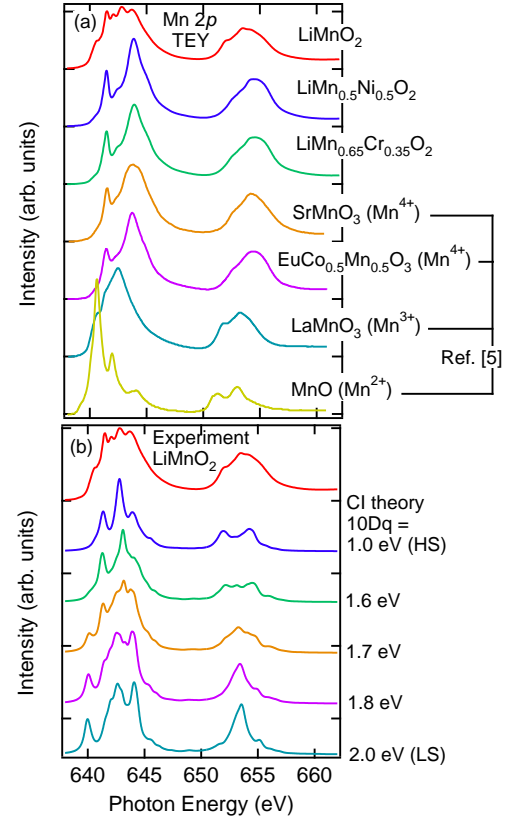


FIG. 2: (Color online) (a) Mn 2*p* XAS spectra and their comparison with the reference data of Mn²⁺ (MnO), Mn³⁺ (LaMnO₃), and Mn⁴⁺ (EuCo_{0.5}Mn_{0.5}O₃ and SrMnO₃) from Ref. [5]. (b) Comparison with the CI theory.

10*Dq* means that *e_g* states have a higher energy than *t_{2g}*, which is the case in the MnO₆ octahedral coordination as shown in Fig. 1 (a) [7]. The increase of 10*Dq* from 1.0 eV to 2.0 eV corresponds to the transition from HS to LS states. (The electron configurations are shown in Fig. 1 (b)). The spectrum of LaMnO₃ in Fig. 2 (a) is in good agreement with the results of CI theory with 10*Dq* = 1.0 or 1.6 eV, which shows that Mn³⁺ in LaMnO₃ is in the HS state, consistent with the reported result [8]. The spectrum of LiMnO₂ in Fig. 2 (a) is in good agreement with the CI theory of 10*Dq* = 1.7 eV. This result demonstrates that the Mn³⁺ in LiMnO₂ is a mixture of the HS and LS states, consistent with the result from a similar analysis by de Groot [9]. If the 10*Dq* value of LiMnO₂ is slightly increased by chemical substitution, substrate strain etc., then the Mn³⁺ LS state can be realized in LiMnO₂, as predicted by first-principle calculations [3].

We also determined the valence of Ni and Cr by XAS spectra. Figure 3 shows the Ni 2*p* XAS spectrum of LiMn_{0.5}Ni_{0.5}O₂ and its comparison with the reference data of Ni²⁺ (NiO) and Ni³⁺ (NdNiO₃ and PrNiO₃) from Ref. [10]. The spectrum of LiMn_{0.5}Ni_{0.5}O₂ is similar

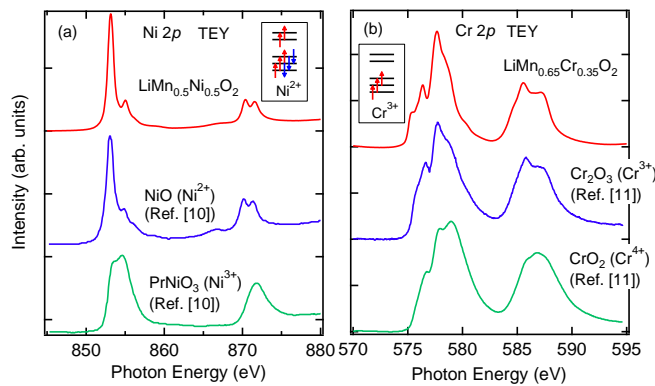


FIG. 3: (Color online) (a) Ni 2p XAS spectrum of $\text{LiMn}_{0.5}\text{Ni}_{0.5}\text{O}_2$ and its comparison with the reference data of Ni^{2+} (NiO) and Ni^{3+} (NdNiO_3 and PrNiO_3) from Ref. [10]. The inset shows the electron configuration of Ni^{2+} . (b) Cr 2p XAS spectrum of $\text{LiMn}_{0.65}\text{Cr}_{0.35}\text{O}_2$ and its comparison with the reference data of Cr^{3+} (Cr_2O_3) and Cr^{4+} (CrO_2) from Ref. [11]. The inset shows the electron configuration of Cr^{3+} .

to that of NiO rather than NdNiO_3 and PrNiO_3 , indicating that the valence of Ni is 2+ in $\text{LiMn}_{0.5}\text{Ni}_{0.5}\text{O}_2$. Similarly, it is shown from the Cr 2p XAS spectrum of $\text{LiMn}_{0.65}\text{Cr}_{0.35}\text{O}_2$ Fig. ?? and its comparison with the reference data of Cr^{3+} (Cr_2O_3) and Cr^{4+} (CrO_2) from Ref. [11] that our result is similar to that of Cr_2O_3 and the valence of Cr is 3+ in $\text{LiMn}_{0.65}\text{Cr}_{0.35}\text{O}_2$.

From the above results, we determined that the electronic configurations in powder samples are $\text{LiMn}^{3+}\text{O}_2$, $\text{LiMn}_{0.5}\text{Ni}_{0.5}\text{O}_2$, and $\text{Li}_x\text{Mn}_{0.65}\text{Cr}_{0.35}\text{O}_2$. In the Cr-substituted sample, we have to take into account the Li deficiencies to keep the material charge-neutral, and the value of Li concentration x is calculated to be 0.35. Such a large Li deficiency is also concluded from the results of photoemission spectroscopy [12].

When we substitute Cr for Mn in LiMnO_2 , the Cr^{3+} valence and the change from Mn^{3+} to Mn^{4+} introduce Li deficiencies and make this material unsuitable for battery cathodes. In the case of Ni substitution, the Ni^{2+} valence and the change from Mn^{3+} to Mn^{4+} do not create Li deficiencies and the material is suitable for cathodes. When we classify transition-metal compounds in the scheme of Zaanen, Sawatzky and Allen [13, 14], that is as a function of Coulomb repulsion U and charge-transfer energy from O 2p states to transition-metal 2p states Δ , charge-transfer-type ($\Delta < U$) such as Ni and Cu is more suitable for LiMnO_2 battery cathodes than Mott-Hubbard type ($U < \Delta$) such as Cr because Ni and Cu becomes 2+ and does not cause Li-deficiencies in the material.

We performed an x-ray absorption study of LiMnO_2 and its related materials and determined the oxidation states of transition-metal ions. The XAS result of LiMnO_2 shows that the Mn^{3+} in LiMnO_2 is a mixture of the HS and LS states, suggesting that small perturba-

tion such as Cr doping in powder samples or substrate strain of thin films may stabilize the LS Mn^{3+} state in LiMnO_2 . In $\text{Li}_x\text{Mn}_{0.65}\text{Cr}_{0.35}\text{O}_2$, although the substituted Cr becomes 3+ as expected, the Cr doping unfortunately causes Li deficiencies and introduces Mn^{4+} . In contrast, $\text{LiMn}_{0.5}\text{Ni}_{0.5}\text{O}_2$ has substituted Ni of 2+ and does not include Li deficiencies. Thus we conclude that the substitution of charge-transfer-type Ni or Cu is effective for LiMnO_2 battery materials.

This research was made possible with financial support from the Canadian funding organizations NSERC, CFI, and CIFAR.

* Electronic address: wadati@phas.ubc.ca;
URL: <http://www.geocities.jp/qxbqd097/index2.htm>

- [1] K. Mizushima, P. C. Jones, P. J. Wiseman, and J. B. Goodenough, *Mater. Res. Bull.* **15**, 783 (1980).
- [2] K. Kang, Y. S. Meng, J. Breger, C. P. Grey, and G. Ceder, *Science* **311**, 977 (2006).
- [3] Z.-F. Huang, F. Du, C.-Z. Wang, D.-P. Wang, and G. Chen, *Phys. Rev. B* **75**, 054411 (2007).
- [4] F. Du, Z.-F. Huang, C.-Z. Wang, X. Meng, G. Chen, Y. Chen, and S.-H. Feng, *J. Appl. Phys.* **102**, 113906 (2007).
- [5] A. N. Vasiliev, O. S. Volkova, L. S. Lobanovskii, I. O. Troyanchuk, Z. Hu, L. H. Tjeng, D. I. Khomskii, H.-J. Lin, C. T. Chen, N. Tristan, F. Kretzschmar, R. Klingeler, and B. Buchner, *Phys. Rev. B* **77**, 104442 (2008).
- [6] A. Tanaka, *J. Phys. Soc. Jpn.* **63**, 2788 (1994).
- [7] Based on the crystal structure of these materials, the Mn ion is in a trigonal symmetry, but since the trigonal distortion is small, we consider it a reasonable approximation to calculate using an octahedral symmetry. The parameters in the calculation are the charge-transfer energy from the O 2p orbitals to the empty Mn 3d orbitals $\Delta = 4.5$ eV, the 3d - 3d on-site Coulomb interaction energy denoted $U = 4.0$ eV, and the hybridization strength between the Mn 3d and O 2p orbitals $V(e_g) = 3.0$ eV.
- [8] M. Abbate, F. M. F. de Groot, J. C. Fuggle, A. Fujimori, O. Strebel, F. Lopez, M. Domke, G. Kaindl, G. A. Sawatzky, M. Takano, Y. Takeda, H. Eisaki, and S. Uchida, *Phys. Rev. B* **46**, 4511 (1992).
- [9] F. M. F. de Groot, *J. Electron Spectrosc. Relat. Phenom.* **61**, 529 (1994).
- [10] M. Medarde, A. Fontaine, J. L. Garcia-Munoz, J. Rodriguez-Carvajal, M. de Santis, M. Sacchi, G. Rossi, and P. Lacorre, *Phys. Rev. B* **46**, 14975 (1992).
- [11] Y. S. Dedkov, A. S. Vinogradov, M. Fonin, C. Konig, D. V. Vyalikh, A. B. Preobrajenski, S. A. Krasnikov, E. Y. Kleimenov, M. A. Nesterov, U. Rudiger, S. L. Molodtsov, and G. Guntherodt, *Phys. Rev. B* **72**, 060401 (2005).
- [12] N. Takaiwa *et al.*, private communication.
- [13] J. Zaanen, G. A. Sawatzky, and J. W. Allen, *Phys. Rev. Lett.* **55**, 418 (1985).
- [14] A. E. Bocquet, T. Mizokawa, K. Morikawa, A. Fujimori, S. R. Barman, K. Maiti, D. D. Sarma, Y. Tokura, and M. Onoda, *Phys. Rev. B* **53**, 1161 (1996).